

# Fractal Signature Feature Analysis of MODIS NDVI Time Series Data

Shi-Wei Dong, Hong Li and Wei-Wei Zhang

*Beijing Academy of Agriculture and Forestry Sciences, Beijing Research and Development Center for Grass and Environment, 100097 Beijing, China*

**Abstract.** Fractal signature feature of MODIS Normalized Difference Vegetation Index (NDVI) time series data is proposed in this study in order to further mine its inherent information. Savitzky-Golay filter is adopted to reconstruct MODIS NDVI time series curves of Beijing in China. The blanket method used for computing fractal dimension of surface is modified and then transferred to compute upper and lower fractal signature of each pixel in NDVI time series images. The fractal signature and their corresponding scale are analyzed, and the results show that fractal signature curves and fractal signature images can clearly reflect different targets of land use and land cover at certain scales. This study also provides a new secondary characteristic parameter for related studies.

## 1 Introduction

Normalized Difference Vegetation Index (NDVI) time series data acquired by the satellite sensors can accurately reflect the dynamic state and seasonal variation characteristics of the vegetation [1]. It plays an important role in the range of global, continental and regional vegetation cover mapping, land cover monitoring, ecosystem dynamic monitoring and simulation, crop growth monitoring, crop yield estimation and other aspects.

Fractal theory is a very efficient method to depict chaotic, erratic, and natural phenomena [2]. After Mandelbrot [3] introduced the notion of fractals in the 1970s, fractal theory was applied to numerous domains like image segmentation [4, 5] and texture analysis [6]. Many articles have discussed the issue of fractal-based processing and interpretation of remote sensing image [7, 8]. When fractal signatures are applied in image analysis, fractal dimension is first chose to calculate. Many methods exist to compute fractal dimension and are grouped into three classes: (1) box-counting methods, e.g. the differential box-counting method [9], (2) fractional Brownian motion methods, e.g. the power spectrum [10], and (3) area measurement methods, e.g. the blanket method [11].

The scale is greatly significant in NDVI time series images processing and there is an optimum observed scale for each land use and land cover type. The same ground target may be exhibited differently in remote sensing image under different scales [12]. In MODIS images, each pixel has a NDVI time series curve whose shape depends on specific target. Different target in land use and land cover must have different fractal dimension. Therefore, the objectives of this study are to try to introduce and analyze fractal signature feature of MODIS

NDVI time series data in order to obtain optimum observed scales of different targets from fractal signature curves and fractal signature images. It is playing a very important role in image processing, feature extraction and pattern recognition.

The remainder of this paper is organized as follows. Study area is introduced in the next section. In section 3, experimental data are acquired and processed, and detailed method for fractal signature calculation is briefly presented. MODIS NDVI time series data are processed by fractal computer programs and fractal features are specifically analyzed in section 4. Finally, discussion and conclusions of this study are extracted in section 5 and 6, respectively.

## 2 Study Area

Beijing is located in the northwest of the North China Plain between longitude 115°25'-117°30' E and latitude 39°28'-41°05' N (Figure 1), and has an estimated area of 16,410 km<sup>2</sup>. Hills and mountains in the northwest account for 62% of the entire area while plains in the southeast cover the remaining 38%, and the average elevation of Beijing is 43.5 m. The area belongs to the warm temperate semi-humid continental monsoon climate with an average annual temperature is 12.5°C, and the average precipitation is 566.1 mm. Beijing's population rose to 20.69 million in 2012.

The primary land use and land cover types in the area are divided into five general categories, including cropland, construction, forest, water and orchard. Additionally, agricultural cropping patterns in Beijing are dominated by double cropping and single cropping. The overwhelming majority of crops with double cropping are

winter wheat-summer corn. Crops with single cropping are primarily spring corn or winter wheat.

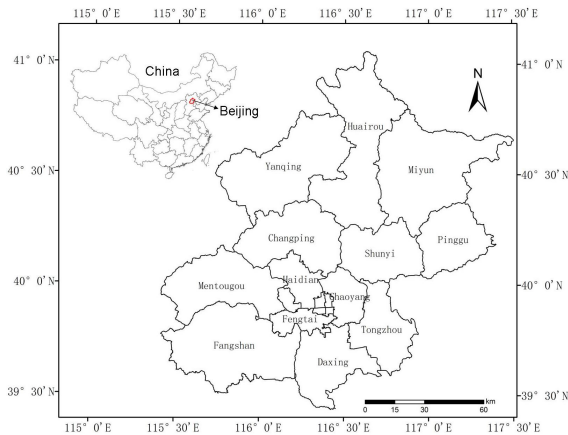


Figure 1. Study Area.

### 3 Data and Method

#### 3.1 Data Acquisition and Processing

In this study, MOD09 MODIS product consisted of eight days of composite surface reflectance images are primarily employed, and they are freely available from the MODIS data product website (<http://modis.gsfc.nasa.gov>). A set of 46 time-phase images of Beijing (h26v04 and h26v05) can cover a full year observation period from Jan.1, 2007 to Jan.3, 2008. File formatting conversion and projection conversion are implemented by MODIS Reprojection Tool.

The NDVI produced at 250 m resolution from MODIS is normalized difference measure comparing the near infrared (846-885 nm) and visible red (600-680 nm) bands. Some noise derived from clouds and the atmosphere are detrimental to the trends analysis and information extraction, so the Savitzky-Golay filter [13] is used to obtain high-quality NDVI time series in this study, and the reconstructed NDVI time series can much more clearly reflect the trends and regularity in vegetation activity.

#### 3.2 Method

Peleg et al [11] defined fractal signature as the change in measured area with changing scale and proposed blanket method to computer spatial fractal dimension of remote sensing image. The principle of this method is that a remote sensing image is treated as a 3-D topography, and the gray of each pixel as height. The terrain surface is then enveloped by two blankets on the each side with a distance of  $\epsilon$ , the fractal dimension of the image can be computed by the relation between the area of the blankets and the volume of the space enveloped by the two blankets. 2-D curve can be considered as a special kind of 3-D ground surface, and the length of the 2-D curve as the 3-D terrain surface while the area enclosed by 2-D curve as the volume of the space enveloped by 3-D

topography. Thus, this method is modified and then transferred to compute fractal dimension of MODIS NDVI time series curve.

## 4 Results and Analysis

### 4.1 Fractal Processing

Fractal computer programs are developed using the visualization interactive data language ENVI/IDL programming. MODIS NDVI time series data of Beijing are processed by this programming to obtain upper and lower fractal profiles. Different fractal signal images can be obtained after fractal processing with different values of measure scale. Pixel signal value in each fractal image reflects the complexity of the variation of the NDVI time series curve at certain scale. When the pixel signal value in fractal signature image is much higher, the NDVI time series curve has much more complex variation. Scale with the highest signal value and most obvious distinguish with other targets in fractal image is defined as fractal feature scale of this target.

### 4.2 Fractal Feature Analysis

#### 4.2.1 Fractal Signature Curves

Figure 2-7 are the fractal signature curves with scale  $\epsilon$  from 2 to 30 for upper and lower profiles of MODIS NDVI time series data in Beijing. We can find that typical targets can be clearly reflected at different fractal scale of upper and lower fractal profiles. Fractal feature scale of single cropping cropland is located in the upper fractal profiles at  $\epsilon=23$ , Figure 2. Fractal feature scales of double cropping cropland are located in the upper fractal profiles at  $\epsilon=12$  and the lower fractal profiles at  $\epsilon=5$ , Figure 3. Fractal feature scales of construction are located in the upper fractal profiles at  $\epsilon=14$  and the lower fractal profiles at  $\epsilon=16$ , Figure 4. Fractal feature scales of forest are located in the upper fractal profiles at  $\epsilon=15$  and the lower fractal profiles at  $\epsilon=11$ , Figure 5. Fractal feature scale of water is located in the upper fractal profiles at  $\epsilon=22$ , Figure 6. Fractal feature scales of orchard are located in the upper fractal profiles at  $\epsilon=23$  and the lower fractal profiles at  $\epsilon=12$ , Figure 7.

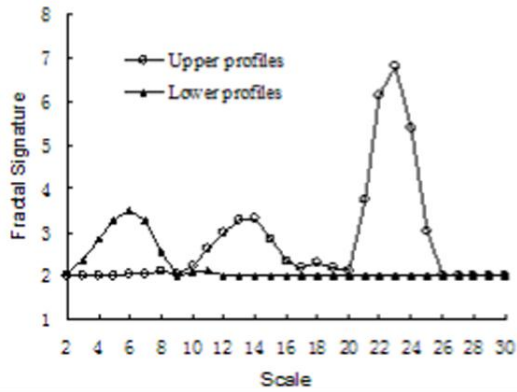


Figure 2. Fractal Signature Curves of Single Cropping Cropland.

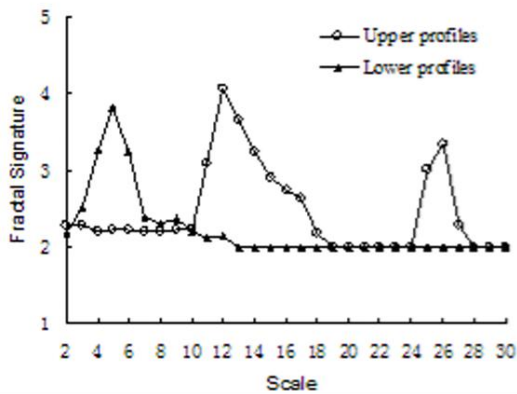


Figure 3. Fractal Signature Curves of Double Cropping Cropland.

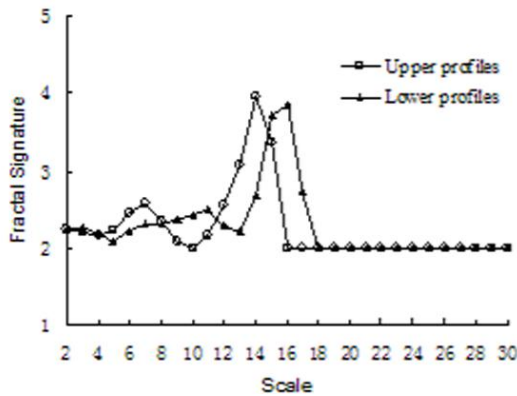


Figure 4. Fractal Signature Curves of Construction.

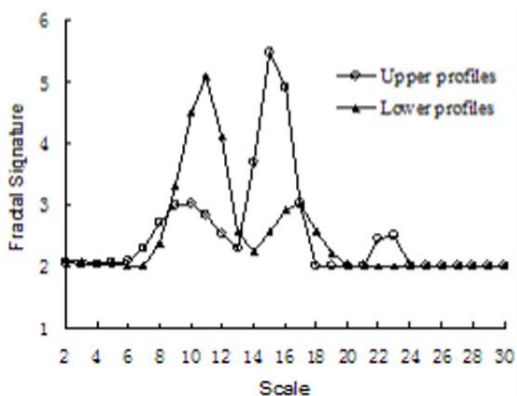


Figure 5. Fractal Signature Curves of Forest.

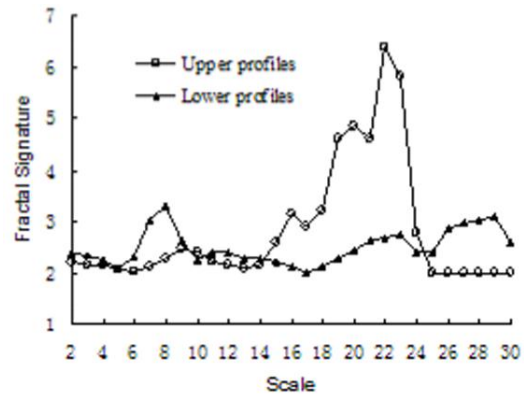


Figure 6. Fractal Signature Curves of Water.

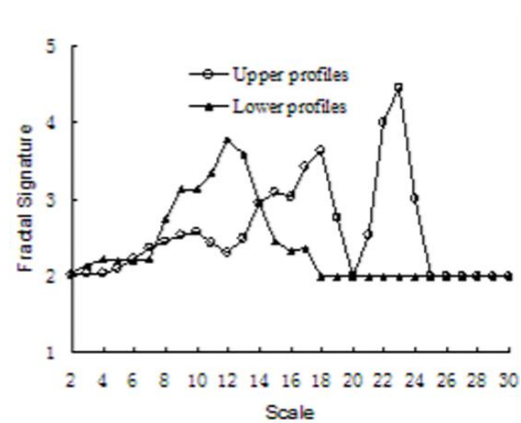


Figure 7. Fractal Signature Curves of Orchard.

In a word, different targets exhibit different fractal feature, and fractal signature can distinguish targets more effectively than the original data.

#### 4.2.2 Fractal Signature Images

Figure 8-11 are fractal signature images obtained from upper fractal at  $\epsilon=4$  and  $\epsilon=23$ , lower fractal at  $\epsilon=5$  and  $\epsilon=11$ . Brightness in the image is on behalf of the value of fractal signal strength, and when the pixel is much brighter, the value of fractal signal strength is much higher. Preliminary analyses indicate that the fractal signature images can also reflect the land use and land cover types. Construction and water have relatively brighter tones in Figure 8. Single cropping cropland and orchard are reflected in Figure 9, which are in accord with the results from fractal signature curves in Figure 2 and Figure 7, respectively. Double cropping cropland is revealed in Figure 10, corresponding to the results from fractal signature curves in Figure 3. Correspondingly, forest is exhibited in Figure 11, which also conforms to the results from fractal signature curves in Figure 5.



Figure 8. Upper Fractal Image of  $\varepsilon=4$ .



Figure 9. Upper Fractal Image of  $E=23$ .



Figure 10. Lower Fractal Image of  $\varepsilon=5$ .

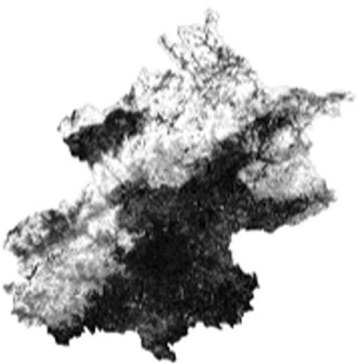


Figure 11. Lower Fractal Image of  $\varepsilon=11$ .

## 5 Discussion

Fractal signature feature of MODIS NDVI time series can reveal obvious differences in land use and land cover types at certain scales. This results are consistent with previous studies in recent years. Different targets can be characterized by fractal feature scale in reference [12]. Higher precision of classification may be expected based on fractal feature. The result shows that the overall accuracy with fractal-based textures increased 5.31% in reference [14].

## 6 Conclusions

This study provided a new secondary characteristic parameter of MODIS NDVI time series namely fractal signature, which was great benefit to image classification, pattern recognition, texture analysis and image segmentation, especially for low spatial resolution remote sensing images. The results showed that fractal signature feature of MODIS NDVI time series can reveal obvious differences in land use and land cover types at certain scales. Fractal feature scales of different targets were proposed based on analysing from fractal signature curves and fractal signature images.

In addition, the relation between fractal signature value and target types were not clear in this study. The fractal signature used for quantitative interpretation of remote sensing data was discussed in further research.

## Acknowledgments

This work was supported by the Beijing Excellent Talent Support program (No. 2015000020060G136) and Beijing Science and Technology Programs.

## References

1. M. Rees, R. Condit, M. Crawley, S. Pacala and D. Tilman, *Science* 293, 5530 (2001)
2. M. G. Hu, J. F. Wang and Y. Ge, *Sensors* 9, 11 (2009)
3. B. B. Mandelbrot and M. Aizenman, *Phys. Today* 32, 65 (1979)
4. Y. Xia, D. Feng and R. Zhao, *IEEE Trans. Image Process.* 15, 3 (2006)
5. Q. Guo, J. Shao, F. Guo and V. Ruiz, *Int. J. Comput. Ass. Rad.* 2 (2007)
6. M. P. Bishop, J. F. Shroder Jr, B. L. Hickman and L. Copland, *Geomorphology* 21, 3 (1998)
7. W. Sun, G. Xu, P. Gong and S. Liang, *Int. J. Remote. Sens.* 27, 22 (2006)
8. R. Lopes and N. Betrouni, *Med. Image Anal.* 13, 4 (2009)
9. B. B. Chaudhuri and N. Sarkar, *IEEE T. Pattern Anal.* 17, 1 (1995)
10. A. P. Pentland, *IEEE T. Pattern Anal.* 6 (1984)
11. S. Peleg, J. Naor, R. Hartley and D. Avnir, *IEEE T. Pattern Anal.* 4 (1984)
12. Z. Zhou and Q. Bu, *Yaogan Xuebao- J. Remote Sens.* 15, 1 (2011)

13. A. Savitzky and M. J. E. Golay, *Anal. Chem.* 36, 8 (1964)
14. S.Zheng, J. Zheng, M. Shi, et al, *Yaogan Xuebao- J. Remote Sens.* 18, 4 (2014)